

Estimation of the error of representivity for AIRS observations

J.R.N. Cameron



SUMMARY: High resolution infra-red instruments generally have several thousand channels, the weighting functions of which significantly overlap. Extracting the full vertical resolution from these measurements while not introducing noise may require a careful treatment of the statistics of channel differences. It is therefore desirable to be aware of the magnitude and structure of the observation error, which is made up of the instrument error, forward model error and errors of representivity.

The error of representivity for AIRS observations in the context of a global model data assimilation system is investigated using the observational (or Hollingsworth-Lönnberg) method of studying the covariance of nearby, cloud-free fields-of-view for different spatial separations.

1. Method

Accurate numerical weather forecasts rely upon an accurate initial analysis. At the Met Office, the initial analysis is created by combining meteorological observations from around the world with the forecast fields from the previous data assimilation and forecast cycle. To find a combination that is close to optimal, a variational technique is used that searches for a small perturbation to the first guess analysis that results in a best fit to the observations and the forecast field. A prospective analysis field may be compared to satellite radiances through the use of a forward model. The forward model computes the satellite radiances that would be expected from a given field. Differences between the actual and simulated radiances arise from various sources: the model field error; the forward model error; the instrument noise; and errors of representivity (instrumental error is usually lumped together with forward model error and treated as a single bias). Errors of representivity account for the different spatial scales that the real and simulated observations describe. AIRS observations, for example, have a footprint of about 14 km. Simulated observations are derived from model fields and model fields cannot have horizontal structure on scales finer than a grid box. Grid boxes are approximately 60 km square in the Met Office global model. In practice, the highest spatial frequency that a model can represent is somewhat larger than a grid box. Figure 1 illustrates the various sources of error that contribute to the difference between observed and simulated radiances.

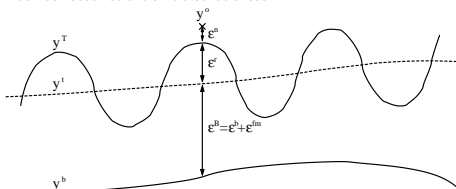


Figure 1: A diagram of the various errors that contribute to the difference between a real, y^t , and simulated, y^s , satellite observation. The true radiance is depicted as y^t and the true radiance smoothed to the scale hoped to be achieved in the analysis is y^s . ϵ^i is the instrument noise, ϵ^r is the error of representivity, ϵ^b is the background error and ϵ^{fm} is the forward model error.

It is possible to partially separate the various contributions to the difference between observed and background (simulated) radiances through their different horizontal correlations. This approach is known as the observational (or Hollingsworth-Lönnberg) method. Let the observed minus background radiance for observation x and channel i be denoted by delta:

$$\Delta_{x,i} = O_{x,i} - B_{x,i}$$

To separate out the contributions, the covariance of delta for two channels at different locations must be compared to the covariance of delta at the same location:

$$\text{cov}(\Delta_{x,i}, \Delta_{y,j}) \Big|_{x=y} - \text{cov}(\Delta_{x,i}, \Delta_{y,j}) \Big|_{x \neq y} \quad (1)$$

The first term in this equation includes contributions from every source of error because it is evaluated for the same observation and so all differences are projected out. The second term only includes those errors that co-vary over the spatial separation between observation x and y . Assuming the different error contributions do not co-vary with one another, the above equation may be expanded to:

$$\begin{aligned} \text{cov}(\epsilon_{x,i}^n, \epsilon_{y,j}^n) \Big|_{x=y} - \text{cov}(\epsilon_{x,i}^n, \epsilon_{y,j}^n) \Big|_{x \neq y} + \\ \text{cov}(\epsilon_{x,i}^r, \epsilon_{y,j}^r) \Big|_{x=y} - \text{cov}(\epsilon_{x,i}^r, \epsilon_{y,j}^r) \Big|_{x \neq y} + \\ \text{cov}(\epsilon_{x,i}^b, \epsilon_{y,j}^b) \Big|_{x=y} - \text{cov}(\epsilon_{x,i}^b, \epsilon_{y,j}^b) \Big|_{x \neq y} \quad (2) \end{aligned}$$

Observe that the second term in this equation is always zero, since the instrument noise is independent for different observations.

The two terms in equation 1 may be computed from pairs of cloud-free observations and the pairs may be selected such that they all have a similar separation. For pairs separated by a very short distance, the error of representivity and background error will almost be the same in both observations, so terms 3 and 4 and terms 5 and 6 will cancel in equation 2,

leaving only the instrument noise. For separations a little larger than the grid scale, the error of representivity will be unrelated for the two observations, and term 4 in equation 2 will now be zero. At this separation, equation 1 will equal the instrument noise plus the error of representivity. At very large separations, the background error of the two observations will become unrelated and terms 2, 4 and 6 in equation 2 will be zero. Equation 1 at this separation will be the covariance of observed minus background.

2. Results

Statistics to form the two terms in equation 1 were collected for pairs of cloud-free observations and this was repeated for a range of pair separations. The statistics for channels in the short wavelength band do not include any day-time fields-of-view. The data was from April 2005 and, typically, 5000 pairs of observations were collected for each separation. The shortest separation studied was 75 km. Pairs of observations with small separations are strongly biased towards the centre of the scan.

Figure 2 shows a typical AIRS spectrum plotted against frequency and channel index. Channel index is used to identify channels in all subsequent figures. The variances are all plotted in units of brightness temperature squared. Figures 3, 4, 5 and 6 present various aspects of the accumulated statistics (see the legends for details). A simple interpretation of these figures is complicated by the fact that, in the Met Office system, the background skin temperature of the surface used at the data assimilation stage is derived from an initial single column retrieval. This value of skin temperature is therefore representative of the observation and not the grid box. The value of background skin temperature used to create these plots was taken from the model background, resulting in a representivity error and covariances between the surface channels which will not be relevant to data assimilation. The highly correlated structure in the water vapour band is the most significant result from the perspective of data assimilation.

Note that the observational method is equally applicable to channel radiances, reconstructed radiances and eigenvector weights. It would be possible, for example, to derive the full observation error covariance matrix of IASI principle components from raw data, provided that the observations were close enough together to neglect errors of representivity.

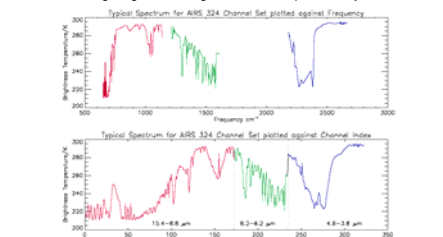


Figure 2: The AIRS 324 channel set against frequency and channel index. Channel index is used in all subsequent figures

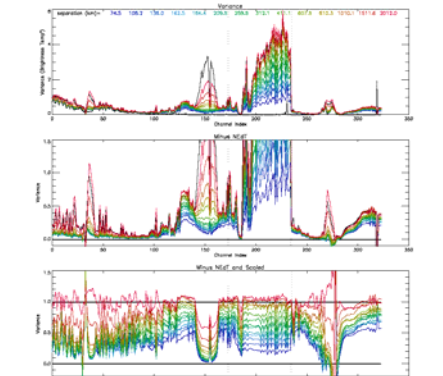


Figure 3: The error variance, as defined in equation 1, for different spatial separations. The shortest separations are in blue and the longest in red. The lower solid black line is the instrument error from calibration and the upper black line is the variance of observed minus background for randomly chosen observations. In the middle plot, instrument error has been subtracted from all lines. In the lower plot, instrument error has been subtracted and the resulting values scaled by the variance of observed minus background. For small separations, variance will be dominated by instrument noise plus representivity error. Error variance is expected to tend towards the variance of observed minus background at large separations

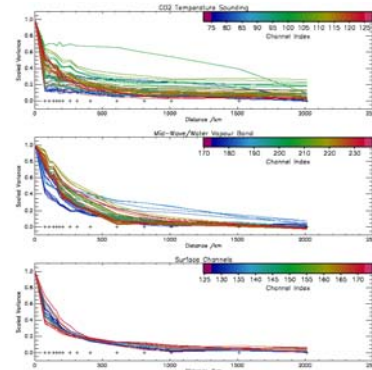


Figure 4: The covariance of observed minus background for observations at different separations scaled by the variance of observed minus background at zero separation. The three figures show channels sensitive to atmospheric temperature, water vapour and the surface respectively. The value at zero distance is from the observed minus background for randomly chosen observations and is the same as the first term in equation 1 in the absence of data selection bias. Values at non-zero distances are from the second term in equation 1. The step between the value at zero distance and the value at 75 km is a measure of the noise plus representivity error. Curves show how rapidly the background error covariance falls with distance

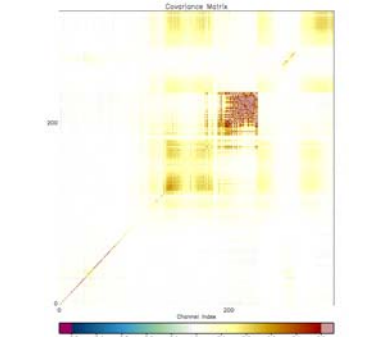


Figure 5: Full covariance matrix for the noise plus representivity error (equation 1 for the smallest separation of 75 km). Detectors in AIRS are independent (assuming there is no cross-talk) so off-diagonal features are due to errors of representivity. The one exception is channel 30, used to extrapolate above the model top. Stratospheric extrapolation complicates interpretation of the plot for all stratospheric channels. The most prominent off-diagonal features are in the water vapour band and remaining features are all in channels sensitive to the surface

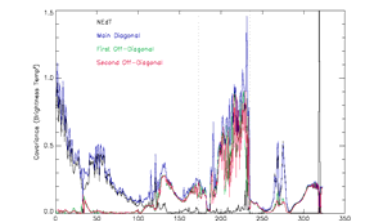


Figure 6: The instrument error is in black and the main diagonal of the covariance matrix in Figure 5 is in blue. The diagonal row either side of the main diagonal is shown in green and the rows either side of that are in red

References

Boutier, F. and Courtillot, P., 1999. Data assimilation concepts and methods. Meteorological Training Course Lecture Series, ECMWF.
http://www.ecmwf.int/newsevents/training/course_notes/DATA_ASSIMILATION/index.html
 Hollingsworth, A., and Lönnberg, P., 1986: The statistical structure of short-range forecast errors as determined from radiosonde data. Part I: The wind field. Tellus, 38A, 111-136.
 Lönnberg, P. and Hollingsworth, A., 1986: The statistical structure of short-range forecast errors as determined from radiosonde data. Part II: The covariance of height and wind errors. Tellus, 38A, 137-161.



Met Office FitzRoy Road Exeter Devon EX1 3PB United Kingdom
 Tel: +44 (0)1392 886902 Fax: +44 (0)1392 885681
 Email: james.cameron@metoffice.gov.uk